Three-dimensional mapping of polarization profiles with thermal pulses

Axel Mellinger,[a] Rajeev Singh,[b] Michael Wegener, Werner Wirges, Reimund Gerhard-Multhaupt, and Sidney B. Lang[c]
Department of Physics, University of Potsdam, Am Neuen Palais 10, D-14469 Potsdam, Germany

(Received 27 September 2004; accepted 6 January 2005; published online 18 February 2005)

High-resolution, large-area three-dimensional mapping of polarization profiles in electret polymers was carried out by means of a fast thermal pulse technique with a focused laser beam. A lateral resolution of 38 μm and a near-surface depth resolution of less than 0.5 μm was achieved. At larger depths, fast thermal diffusion in the metal electrode rather than the laser spot size becomes the limiting factor for the lateral resolution. © *2005 American Institute of Physics*.
[DOI: 10.1063/1.1870124]

During the past three decades, numerous techniques for obtaining space-charge and polarization depth profiles in insulating materials have been developed[1] and applied to a wide range of topics, such as the accumulation of space-charge in high-voltage cable insulations,[2] the development and optimization of pyroelectric and piezoelectric sensors,[3,4] and basic research on the mechanisms of charge storage[5] in electret polymers. Acoustic techniques rely on a pressure step, generated via the absorption of an ultrashort laser pulse[6] or by a fast piezoelectric transducer.[7,8] Alternatively, a short electrical pulse applied to a piezoelectric material or space-charge electret generates a traveling pressure front which can be picked up with a microphone (Pulsed Electro-Acoustic technique, PEA).[9] For thermal techniques, on the other hand, the absorption of a short light pulse (thermal pulse method[10]) or a periodically modulated laser beam (Laser Intensity Modulation Method (LIMM)[11]) by an opaque surface layer causes a time-dependent, spatially varying temperature distribution. In samples that are either pyroelectric or contain an electric space-charge, this gives rise to a short-circuit current, which again carries information on the polarization or space-charge depth profile. All-optical techniques are the method of choice for investigating soft, piezoelectric polymer foams,[12] which are easily deformed upon applying a mechanical stress. In addition, they can be used *in situ* under vacuum conditions.[13]

While most applications of acoustic and thermal profiling techniques yielded one-dimensional distributions, several attempts have been made to obtain two-dimensional surface maps[14] and three-dimensional (tomographic) images, using, e.g., PEA with spatially confined electrodes[15] or acoustic lenses,[16] focused pressure waves[17] and focused LIMM.[3,18] As laser beams can be brought to a tight focus, the latter technique generally achieves a higher lateral resolution than acoustic methods. However, due to the long measurement times (typically several minutes for a complete frequency spectrum), there is generally a trade-off between full spatial resolution with a limited number of beam pointings,[19] or larger, high-resolution area maps at selected modulation frequencies.[20] On the other hand, thermal pulses have recently been shown to yield results similar to LIMM in 1/50 th of the time.[21] In this article, we present a fast three-dimensional mapping technique using thermal pulses generated with a focused laser beam.

The samples were prepared by stretching commercial PVDF films in a hot-zone drawing process at 110 °C with a stretch ratio of 1:4. The resulting films of around 11 μm thickness consist mostly of the polar β phase. For electric poling, both surfaces were metallized with aluminum electrodes of 50 nm thickness, with a "T"-structure at the top and full-area metallization at the bottom. Electric poling was performed in direct contact. In order to control the polarization build-up, the hysteresis of the polarization as a function of the electric field was measured with a setup described in Ref. 22. The coercive field was determined as 50 MV/m. A maximum poling field of 100 MV/m was applied in order to saturate the polarization build-up and to obtain a nearly homogeneous polarization profile across the sample thickness in the metallized area. This poling procedure led to a polarization of ~51 mC/m^2. After poling, the top surface was coated with a full-area copper electrode of 200 nm thickness, which served as laser-absorbing medium. The original "T"-electrode does not significantly alter the thermal properties of the sample and was, therefore, not removed.

The experimental setup is shown in Fig. 1. The second-harmonic beam (wavelength 532 nm) of a Q-switched Nd:YAG laser (Polaris III, New Wave Research) operating at

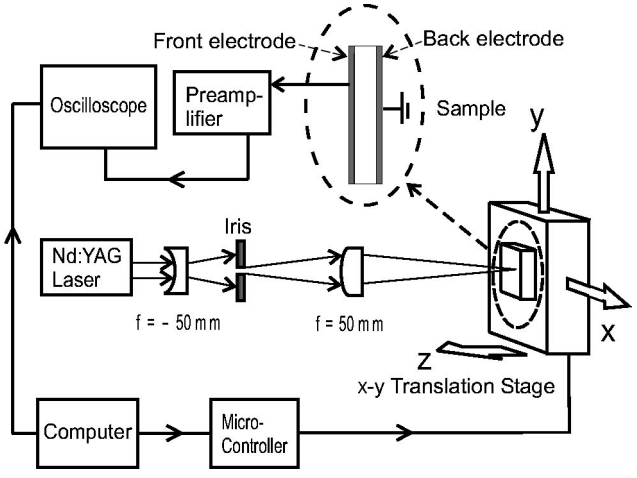

FIG. 1. Experimental setup.

[a]Electronic mail: axm@rz.uni-potsdam.de
[b]Permanent address: Department of Electronics & Communication, University of Allahabad, Allahabad, (U.P.)-211002, India.
[c]Permanent address: Department of Chemical Engineering, Ben-Gurion University of the Negev, P.O.B. 653, 84105 Beer Sheva, Israel.

a repetition rate of 6 Hz was focused onto the polymer film mounted on a computer-controlled *xy* translation stage. By adjusting the *z* position of the sample holder, the laser beam spot size could be varied from 1 mm down to 30 μm, as determined with a knife-edge profiler. The fluence was kept below 0.1 J cm^{-2} to avoid ablation damage.[21] At these low pulse energies, the time-averaged temperature rise in the bulk was well below 1 K. The sample may be either free-standing or attached to a substrate, although the latter is preferred in order to avoid thermo-elastic resonances.[23] The short-circuit pyroelectric or displacement current was amplified by a Stanford Research SR570 current-to-voltage converter and recorded by a digital storage oscilloscope (Agilent 54833A) at a rate of $(\Delta t)^{-1}=10$ MSamples/s. For each beam pointing, 30–50 pulses were averaged and stored on the internal hard disk of the oscilloscope for further processing. The recorded current $I(t_k)$ was Fourier-transformed and divided by the measured (complex) gain spectrum $\tilde{\alpha}(f_n)$ of the SR570 in order to compensate the amplifier-induced signal distortion:

$$\tilde{J}_{\mathrm{exp}}(f_n)=\frac{\Delta t}{\tilde{\alpha}(f_n)}\sum_{k=0}^{N-1} I(t_k)e^{-2\pi ikn/N}. \tag{1}$$

Here, the frequency points are given by

$$f_n=\frac{n}{N\Delta t},\quad n=1\ldots\frac{N}{2}, \tag{2}$$

where $N=512\,000$ is the number of recorded data points.

The computed complex values $\tilde{J}_{\mathrm{exp}}(f_n)$ were analyzed in the same way as conventional LIMM data.[24] The frequency-dependent current $\tilde{J}_{\mathrm{calc}}$ is calculated via the LIMM equation

$$\tilde{J}_{\mathrm{calc}}(f_n)=\frac{A}{d}\alpha_P\int_0^d P(z)\frac{\partial\tilde{T}(z,f_n)}{\partial t}\mathrm{d}z, \tag{3}$$

where A, z, d, and α_P are the irradiated area, depth coordinate, sample thickness, and the relative temperature dependence of the polarization, respectively. The time derivative of the complex temperature $\tilde{T}(z,f_n)$ was computed by solving the one-dimensional heat conduction equation. $P(z)$ is the unknown polarization distribution. This equation is a Fredholm integral equation of the first kind and is "ill-conditioned" with multiple solutions. The correct solution is found by imposing the physical requirement of smoothness on the calculated polarization profile. This is accomplished using the polynomial regularization method (PRM).[24] The polarization distribution was assumed to be an eighth degree polynomial in a normalized logarithmic spatial coordinate $\gamma=(\ln(z)-\ln(z_1))/(\ln(z_2)-\ln(z_1))$:

$$P(\gamma)=a_0\gamma^0+a_1\gamma^1+a_2\gamma^2+a_3\gamma^3+\cdots. \tag{4}$$

Here, z_1 and z_2 are the spatial coordinates of the top electrode–polymer interface and the bottom of the sample, respectively. The coefficients a_i were found by minimizing the function

$$\sum_n \|\tilde{J}_{\mathrm{exp}}(f_n)-\tilde{J}_{\mathrm{calc}}(f_n)\|^2+\alpha^2\int_{z_1}^{z_2}\left(\frac{\mathrm{d}^2P(z)}{\mathrm{d}z^2}\right)\mathrm{d}z, \tag{5}$$

with respect to each of the coefficients. The parameter α is the regularization parameter which controls the smoothness of the solution. It was selected using the L-curve method.[25,26] This analysis was applied to each of the thermal pulse data sets. A near-surface depth resolution of better than 0.5 μm was achieved.

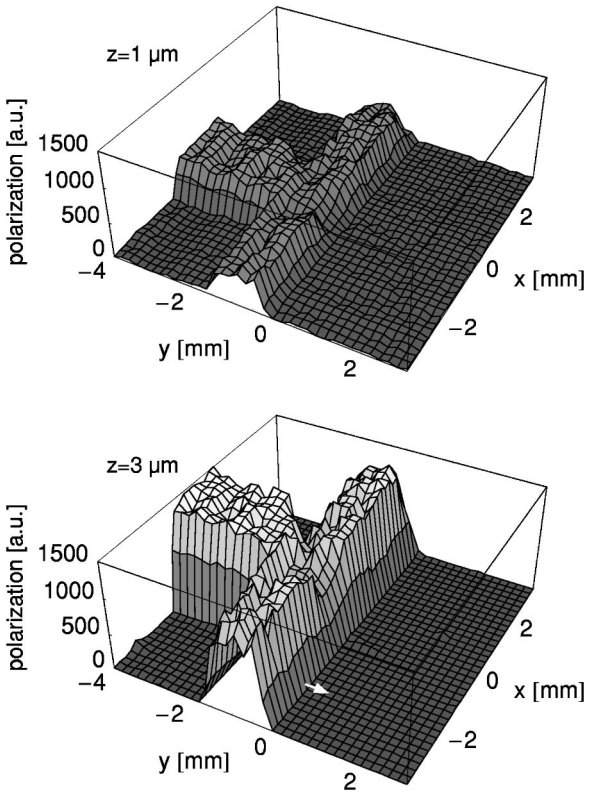

FIG. 2. Polarization map of a 11 μm thick PVDF film poled with a T-shaped electrode. At $z=1$ μm (top graph), the polarization is significantly lower than in the bulk. The arrow indicates the direction of the high-resolution scan shown in Fig. 3.

A polarization map of the PVDF test sample is shown in Fig. 2. The scan covers an area of 7×7 mm^2 with a lateral resolution of 200 μm. Acquisition of the 1296 thermal pulse measurements took ~3.5 h and produced 2 GB of data. The structure of the original "T" electrode is extremely well revealed. Comparing the polarization maps at depths of 1 and 3 μm reveals a substantial edge depolarization, which could be result of impurities. To test the lateral resolution of this method, one-dimensional scans in the *y* direction across the edge of the "T" electrode were performed at the tightest spot size (30 μm). The resulting pyroelectric profile is plotted in Fig. 3 for different depths. At shallow depths ($z=1$ μm), the width of the transition from the poled to the unpoled area is only slightly larger than the spot size, whereas significant broadening to 105 μm is observed at a depth of 4 μm. This reduced lateral resolution can be attributed to the fact that the thermal diffusivity of the metal electrode is approximately three orders of magnitude larger than that of the polymer. As the diffusion length at a time t is given by $s=\sqrt{Dt}$ (where D is the diffusivity), the heated zone will spread out in the electrode some $\sqrt{1000}\approx30$ times faster than in the polymer. Consequently, the resolution at larger depths is limited by thermal diffusion in the electrode, rather than the laser spot size. Nevertheless, it compares favorably with that achieved using acoustic techniques.[16]

In conclusion, we have demonstrated that fast three-dimensional polarization mapping with a near-surface lateral

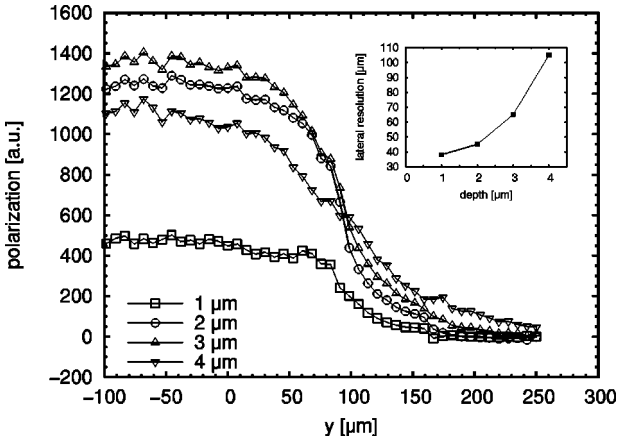

FIG. 3. One-dimensional scan of the polarization distribution in the PVDF sample shown in Fig. 2 at $x=-2.0$ mm and different depths. The lower signal at a depth of 1 μm results from edge depolarization. Fast thermal diffusion in the Cu electrode reduces the lateral resolution at larger depths. The inset shows the width of the transition region measured between 20% and 80% of the plateau height.

resolution of 38 μm can be achieved using the thermal pulse technique. Work is in progress to optimize the thermal properties of the electrode and to model the three-dimensional propagation of the thermal pulse.

The work was funded in part by the European Regional Development Fund. R.S. acknowledges financial support from the German Academic Exchange Service (DAAD). S.B.L. acknowledges financial support during his sabbatical from Ben-Gurion University of the Negev. The authors wish to thank F. Camacho González, R. Flores Suárez, and J.P. Dietrich for their assistance.

[1]S. Bauer and S. Bauer-Gogonea, IEEE Trans. Dielectr. Electr. Insul. **10**, 883 (2003).
[2]K. R. Bambery and R. J. Fleming, IEEE Trans. Dielectr. Electr. Insul. **5**, 103 (1998).
[3]S. Bauer, J. Appl. Phys. **80**, 5531 (1996).
[4]M. Wegener and R. Gerhard-Multhaupt, IEEE Trans. Ultrason. Ferroelectr. Freq. Control **50**, 921 (2004).
[5]A. Mellinger, F. Camacho González, and R. Gerhard-Multhaupt, IEEE Trans. Dielectr. Electr. Insul. **11**, 218 (2004).
[6]G. M. Sessler, J. E. West, R. Gerhard-Multhaupt, and H. von Seggern, IEEE Trans. Nucl. Sci. **29**, 1644 (1982).
[7]W. Eisenmenger and M. Haardt, Solid State Commun. **41**, 917 (1982).
[8]C. Alquié, C. Laburthe Tolra, J. Lewiner, and S. B. Lang, IEEE Trans. Electr. Insul. **27**, 751 (1992).
[9]T. Takada, T. Maeno, and H. Kushibe, in *Proceedings, 5th International Symposium on Electrets* (IEEE Service Center, Piscataway, NJ, 1985), pp. 450–455.
[10]R. Collins, Appl. Phys. Lett. **26**, 675 (1975).
[11]S. B. Lang and D. K. Das-Gupta, Ferroelectrics **39**, 1249 (1981).
[12]J. van Turnhout, R. E. Staal, M. Wübbenhorst, and P. H. de Haan, in *Proceedings, 10th International Symposium on Electrets* (IEEE Service Center, Piscataway, NJ, 1999), pp. 785–788.
[13]A. Mellinger, R. Singh, F. Camacho González, Z. Szamel, and I. Głowacki, in *Proceedings, Conference on Electrical Insulation and Dielectric Phenomena* (IEEE Service Center, Piscataway, NJ, 2004).
[14]C. Alquié, G. Charpak, and J. Lewiner, J. Phys. (Paris), Lett. **43**, L687 (1982).
[15]Y. Imaizumi, K. Suzuki, Y. Tanakoa, and T. Takada, in *Proceedings, International Symposium on Electrical Insulating Materials, Tokyo* (1995), pp. 315–318.
[16]T. Maeno, IEEE Trans. Dielectr. Electr. Insul. **8**, 845 (2001).
[17]X. Qin, K. Suzuki, Y. Tanaka, and T. Takada, J. Phys. D **32**, 157 (1999).
[18]Ş. Yilmaz, S. Bauer, W. Wirges, and R. Gerhard-Multhaupt, Appl. Phys. Lett. **63**, 1724 (1993).
[19]D. Marty-Dessus, L. Berquez, A. Petre, and J. L. Franceschi, J. Phys. D **35**, 3249 (2002).
[20]A. Quintel, J. Hulliger, and M. Wübbenhorst, J. Phys. Chem. B **102**, 4277 (1998).
[21]A. Mellinger, R. Singh, and R. Gerhard-Multhaupt, Rev. Sci. Instrum. **76**, 013903 (2005).
[22]M. Wegener, W. Künstler, K. Richter, and R. Gerhard-Multhaupt, J. Appl. Phys. **92**, 7442 (2002).
[23]P. Bloß, M. Steffen, H. Schäfer, G. M. Yang, and G. M. Sessler, J. Phys. D **30**, 1668 (1997).
[24]S. B. Lang, IEEE Trans. Dielectr. Electr. Insul. **11**, 3 (2004).
[25]S. B. Lang, R. Fleming, and T. Pawlowski, in *Proceedings, Conference on Electrical Insulation and Dielectric Phenomena* (IEEE Service Center, Piscataway, NJ, 2004).
[26]P. C. Hansen and D. P. O'Leary, SIAM J. Sci. Comput. (USA) **14**, 1487 (1993).